JOURNAL OF MATERIALS SCIENCE 27 (1992) 3309–3317

Dynamic modelling of material and process parameter effects on self-propagating high-temperature synthesis of titanium carbide ceramics

A. H. ADVANI
Institute for Manufacturing and Materials Management and Department of Metallurgical and Materials Engineering, University of Texas at El Paso, El Paso, TX 79968, USA

N. N. THADHANI, H. A. GREBE, R. HEAPS, C. COFFIN
Center for Explosives Technology Research, New Mexico Tech, Socorro, NM 87801, USA

T. KOTTKE
Ballistics Research Laboratory, Aberdeen Proving Ground, Aberdeen, Maryland MD 21005, USA

A dynamic, finite-difference model evaluation of titanium carbide (TiC) ceramic processing by self-propagation high-temperature synthesis (SHS) has revealed that material and process parameters have a significant influence on SHS reaction propagation kinetics. Examination of the effects of Ti:C stoichiometry variations and the presence of pre-reacted TiC diluents in the initial (Ti + C) reactant powder mix indicates that off-stoichiometric ratios and dilution additions tend to lower SHS reaction velocities. Increasing compact preheat temperatures, lowering powder particle sizes and raising compact packing densities, on the other hand, cause a significant increase in this reaction variable. Model results are supported by experimental studies on dilution, stoichiometry and preheat temperature effects on SHS velocity, and other literature data on packing density and particle size effects on this parameter. Simulations also suggest that effects of these initial conditions are due to their influence on adiabatic reaction temperatures and heat transfer patterns produced during the process. Critical selection of initial material and process conditions thus appears to be of vital importance during SHS processing of TiC ceramics.

1. Introduction

Self-propagating high-temperature synthesis (SHS) is a relatively recent, economical and energy-efficient process used for the preparation of structural ceramic and intermetallic materials and composites [1–5]. The SHS method involves initiating a self-sustaining exothermic chemical reaction between constituent elemental powders, which self-propagates to yield the (reaction compound) product phase. Compacts prepared by SHS can, however, contain as high as 50% porosity and extensive cracking due to the initial porosity within the green compact, expansion of the compact during reaction, violent gas expulsion during the chemical reaction and rapid cooling of the compact through the ductile–brittle transition temperature of the ceramic or intermetallic phase [6]. A second-stage consolidation method is, thus, often used in conjunction with the SHS method to prepare high-density, crack-free products [6–8].

One of the important considerations in preparing high-quality products during SHS is the ability to understand and control reaction characteristics through suitable selection of material and process parameters prior to processing [1, 2]. This is critical because tailoring of SHS reaction conditions can be a key to obtaining desired properties of the reaction product, which may contribute towards better processing of the final ceramic or intermetallic component. For example, in several intermetallic-forming SHS systems (Ni–Al, Ni–Ti, Ti–Si), the initial reactant powder mixture needs to be preheated within a furnace to even initiate the SHS reaction and form the desired intermetallic [1, 2, 9–11]. In other situations, where the reaction between the constituent elements is extremely violent, control of the SHS reaction may be sought through dilution [12–14], stoichiometric changes, powder morphology changes [15, 16] and other methods [17]. The selection of these initial material and process variables does, however, require a fundamental understanding of the effect of the selected parameter, with respect to the desired final condition of the product. This is not often easy given the possible combinations of initial parameters, the requirement of precise control of the reaction and the complexity of some material systems such as composites.

0022–2461

While experimental solutions can be developed to select desired initial material and processing conditions during SHS [12–17], they are expensive and not versatile. Instead, a quantitative and fundamental understanding of SHS can be better evaluated through resort to predictive models based on the mechanisms involved in the process [18–23]. In this work, a dynamic, finite-difference heat flow model developed to examine the effects of material and process parameter effects on SHS peak temperatures and reaction velocities is described. The model is essentially an extension of previous efforts on heat flow simulation of SHS [20, 21, 23], and assumes reaction kinetics and diffusion processes to have a minor influence on the reaction synthesis phenomena. Predictions were developed to simulate the effects of initial dilution levels, stoichiometric ratio, preheat temperature, particle size and packing density on SHS of TiC. Model performance was evaluated through suitably designed experimental studies, and other available literature data.

2. Analytical methods and experimental techniques

2.1. Dynamic modelling of SHS

In previous work [23] the SHS set-up was modelled by a two-dimensional mesh based on the cylindrical geometry of the Ti–C powder compact and surrounding fixtures (Fig. 1a). The logic of computations that were used to predict peak reaction temperatures and SHS reaction velocities are described in the flow chart of Fig. 1b. The model initially computed the peak temperature of the reaction, T_{ad}, by assuming adiabatic conditions for the reaction through the relation [13]

$$\Delta H = \int_{T_o}^{T_{ad}} C_p \, dT$$

where ΔH is the heat of reaction (J mol^{-1}), C_p is the (molar) heat capacity of the product phase (J mol^{-1} K^{-1}), dT is the temperature step used in the integration process and T_o is the initial temperature of the reactants (K). A variable cell size, multiple material two-dimensional mesh was then developed, and the maximum allowed time-step to avoid numerical instability calculated, through user-specified dimensions and material properties [24–27]. The reaction was "ignited" by assuming the top cell of the (powder) compact to be at the peak reaction temperature. Heat flow initiated between individual cell boundaries preheated subsequent (powder) cells towards the ignition temperature of the reaction. The temperature change ΔT in time Δt within an individual cell was computed by considering conductive heat exchange of the cell with its ($n = 4$) nearest neighbours (see Fig. 1a), which as a first approximation assumes convective and radiative heat transfer to have a minor influence on the heat flow solution. The solution computes $\Delta T/\Delta t$ through the relation [26]

$$\rho C_p \frac{\Delta T}{\Delta t} = \sum_{n=1}^{n=4} kA \frac{T_n - T_o}{\Delta l}$$

where C_p is the specific heat capacity of the cell (J kg^{-1} K^{-1}), k is the composite thermal conductivity of the cell and the neighbour with which heat is being exchanged (W m^{-1} K^{-1}) [21], A is the area through which heat flow occurs (m^2), T_n is the temperature of neighbouring cell (K), T_o is the initial temperature of the cell (K) and Δl is the distance between cell and neighbour (m). Preheated (powder mix) cells which reached the ignition temperature of the reaction were instantaneously converted to the (reacted) product at the adiabatic reaction temperature, which considers that heat transfer, rather than chemical reaction or diffusion kinetics, is the rate-limiting step in the SHS process. The reaction propagated in a wave-like manner to completion, resulting in the (reacted) product phase. Temperature histories for selected cells and times were obtained as output from the software. Reaction velocities were computed based on the time to ignite two specifically located (powder) meshes maintained at a fixed distance in the mesh design.

Modifications to account for material and process parameter effects on SHS were developed by considering the effects of these variables on the peak adiabatic reaction temperature and the heat transfer rate (Fig. 2). An unfixtured Ti–C powder compact was assumed in the process and the two-dimensional system was converted to a simple one-dimensional situation through selection of a 40×1 mesh array of powder size cells. The cell size was typically 50 μm, unless mentioned otherwise, which yielded a time step in the range of 10^{-5}–10^{-6} s for the heat flow calculations.

The effects of dilution, stoichiometric ratio, preheat, packing density and particle size on SHS of TiC were modelled in this work. Dilution effects on SHS were simulated by considering the addition of 0–50% inert (pre-reacted) TiC diluent to the reactant mixture and modelling its influence on the peak temperature and subsequent heat transfer. Since the diluent does not participate in the reaction, it spreads the heat of reaction ΔH over a larger mass of product (TiC) phase and alters the SHS processing characteristics. Ti:C stoichiometric ratios varying from 1:1 to 1:0.5 were also modelled to dilute the reaction heat by leaving unreacted titanium within the product TiC. Stoichiometric ratio variations, in addition, further reduced the ΔH value due to the reaction of smaller molar fractions of reactant powders. Preheating from room temperature to 1000 °C was modelled to raise the initial compact temperature by adding (external) heat to the reaction process, and also to affect the heat transfer by altering the temperature of the individual cells, T_o, undergoing heat transfer. Packing density and particle size were, however, simulated only to alter the heat transfer characteristics. An increase in packing density β was considered to result in an increase in the mass density ρ of individual cells, as also the perpendicular and parallel (to compaction direction) thermal conductivity values of the cell given by [20]

$$k_{\perp} = 9.12\beta^{4.48} \quad \text{W m}^{-1}\text{K}^{-1}$$

$$k_{\parallel} = 3.43\beta^{3.75} \quad \text{W m}^{-1}\text{K}^{-1}$$

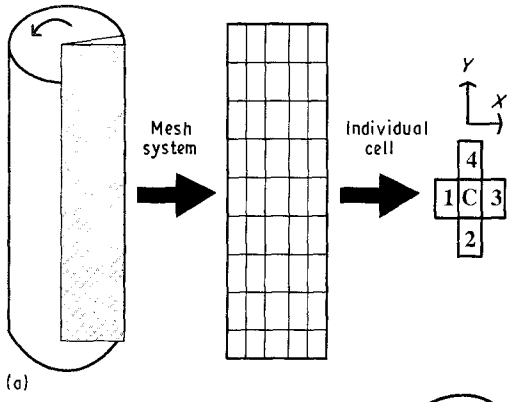

Figure 1 (a) Schematic illustration of two-dimensional mesh set-up showing cell C with its four nearest neighbours and (b) the flow chart used to predict peak reaction temperatures and reaction velocities during SHS. The two-dimensional mesh is a one-degree slice taken from the SHS set-up based on the circumferential nature of the system. The flow chart shows the logic of computations used, and represents data and output files by .dat and .op, respectively.

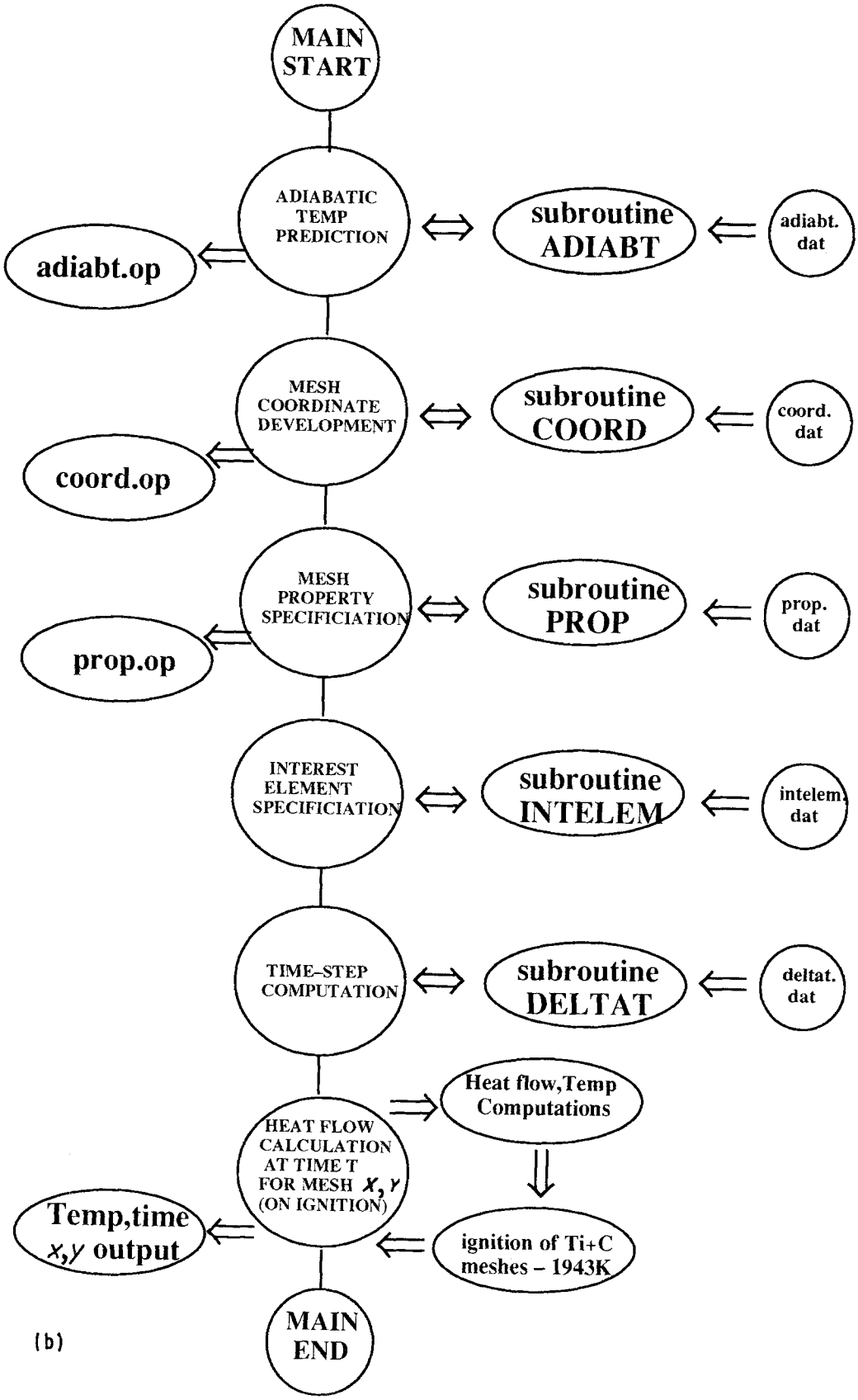

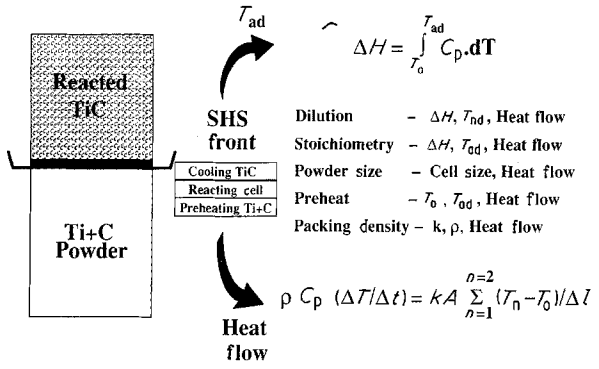

Figure 2 Heat flow and adiabatic temperature modifications used to account for material and process parameter effects on SHS. Note that the SHS front and heat flow calculations only consider two neighbouring cells due to the modified 40 × 1 two-dimensional mesh array used in this work.

Particle size was, on the other hand, modelled by assuming the mesh size to be that of the powder dimension.

2.2. Experimental evaluation of model performance

Model performance was evaluated through experimental verification of dilution, stoichiometric ratio and preheat temperature effects on SHS of TiC, while other available literature on this system was used to evaluate the predictions of packing density and particle size effects on the process. The parameter measured during the experiment was the SHS reaction velocity, which was compared with similar predictions of reaction propagation kinetics obtained from the model.

Measurement of dilution and stoichiometry effects on SHS was carried out using the experimental set-up shown in Fig. 3a. Titanium (44 μm), graphite (2 μm) and pre-reacted titanium carbide (44 μm) powders were weighed to yield the desired stoichiometric ratios (1:1 to 1:0.5 Ti:C) and dilution levels (0–50 wt %). The powders were mixed in a V-blender, and compacted to about 50–55% in 205 mm long, 7 mm diameter plastic straws. Loose Ti–C ignition powder was placed at one end of the compact, into which was inserted an electric match ignition system. The reaction was initiated by igniting the electric match within the loose powder mixture. Once ignited, the reaction self-propagated through the entire compact resulting in the TiC product. The velocity of reaction propagation was measured using two Chromel–Alumel thermocouples placed 68.3 mm apart within the centre of the compact. When the reaction wave passed each thermocouple, a spike corresponding to the shorting-out of the thermocouple was registered on a temperature–time chart recorder. The distance between the thermocouples and the time between temperature spikes yielded the SHS reaction velocity.

The experimental system for measuring preheat effects on SHS velocity was similar to that described above, though the set-up was a little more complex (Fig. 3b). Powders of titanium (44 μm) and graphite (2 μm) were weighed in 1:1 stoichiometric ratios, and mixed in a V-blender system. The powders were packed to about 50–55% density as 125–150 mm long, 10.5 mm diameter rods using an isostatic compaction press, rather than plastic straws, due to the limitation of using the latter within the tube furnace. The ignition system used was a tungsten filament igniter placed within a loose, Ti–C powder mixture as the electric match system was unstable at high furnace temperatures. The compact and ignition system were placed in a sealed tube furnace and argon flow was initiated from one end, while ensuring a positive pressure of the gas at the other end. The argon was required to avoid nitridation of the powders, which was seen to occur at higher preheat temperatures. The sample was slowly heated to the preheat temperature and the reaction was ignited using the tungsten filament wire. Once ignited, the reaction propagated through the compact resulting in titanium carbide product, and the velocity was measured by recording spikes from thermocouples placed 50 mm apart at the centre of the compact. Initial preheat temperatures for which reaction velocities were measured varied from room temperature to a maximum of 1000 °C.

3. Results and discussion

3.1. Dilution and stoichiometry effects on SHS

Simulation of dilution effects on the peak SHS reaction temperature indicated that an increase in the pre-reacted TiC diluent from 0 to 50% resulted in a consistent lowering of the adiabatic reaction temperature (Fig. 4). This reduction in the adiabatic temperature is expected, since the diluent phase is similar to a heat sink, and distributes the heat of reaction to heat both the TiC formed during the reaction and the diluent TiC. The predicted value of adiabatic temperature of 3200 K for undiluted reactant mixtures, and the lowering temperature trend with increasing dilution, are in general agreement with measurements and predictions developed by Holt and Munir [13]. A predicted adiabatic temperature value of 1800 K at 50% dilution level was also noted as unusual, since this value is lower than that of the ignition temperature of 1940 K for the Ti–C SHS reaction.

The lowering of the adiabatic reaction temperature with dilution results in a continuous decrease in the velocity of the SHS reaction due to the slower rates of heat transfer with lower peak temperatures. This reduction in propagation velocity with dilution is illustrated in predictions of temperature–time profiles from two fixed cell locations (Nos 15 and 25, 0.5 mm apart) for 0, 10 and 30% diluent levels (Fig. 5). The plots from the two cells for each dilution level shows an initial slight increase in temperature with time corresponding to the pre-ignition period. Once the reaction within a cell is ignited, a thermal spike to the adiabatic reaction temperature is developed, and rapid cooling of the cell occurs. The stabilization in the temperature gradient after the cooling period appears to be due to heat transfer back from subsequently reacting cells and a limitation of the ignition

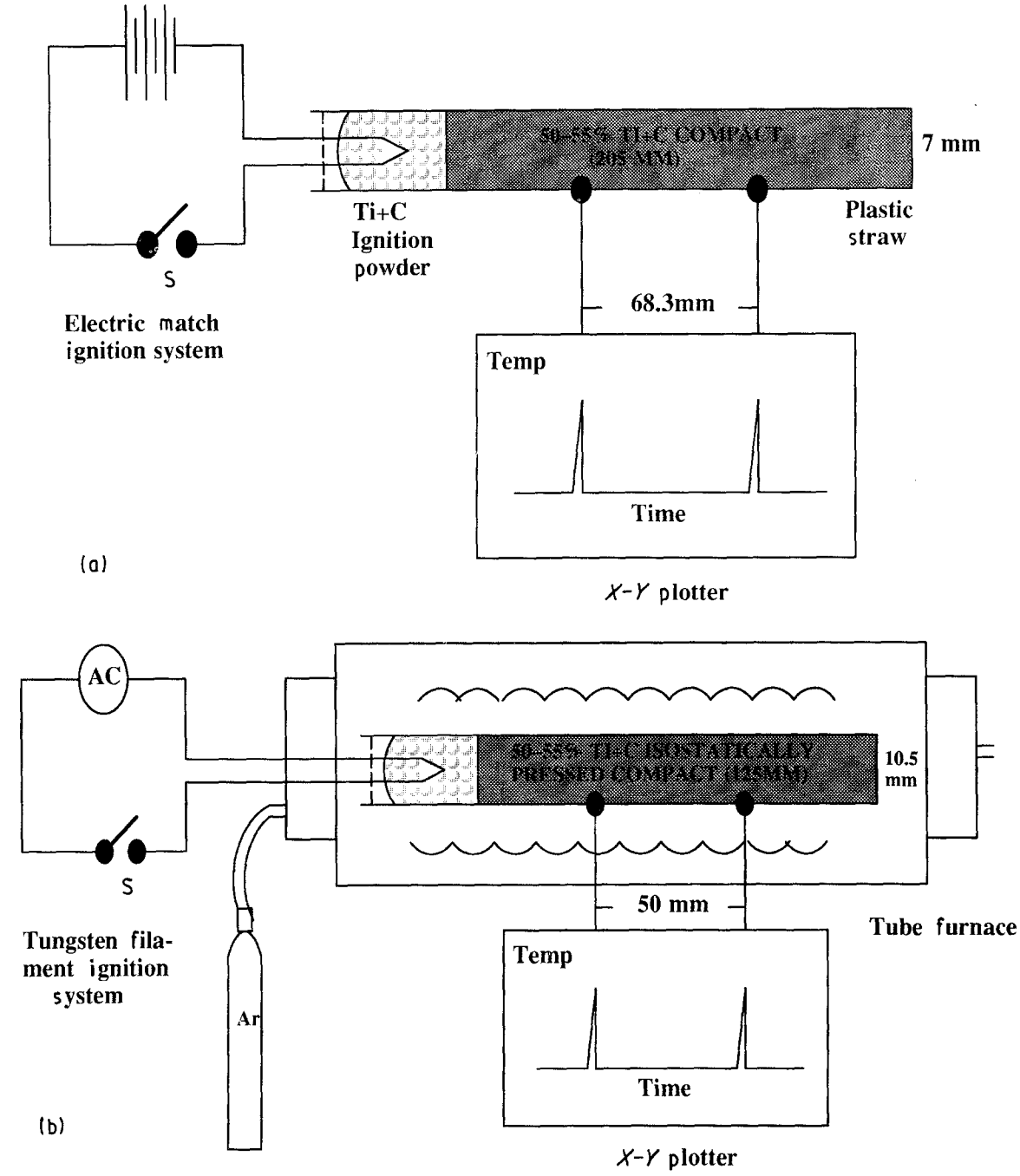

Figure 3 Experimental system used for measurement of (a) dilution and stoichiometry effects and (b) preheat effects on SHS reaction velocity.

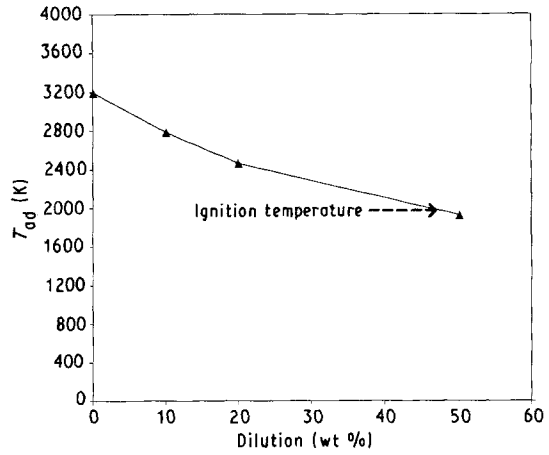

Figure 4 Dilution effects on the adiabatic temperature, indicating a consistent lowering of this peak temperature with a continuous increase in the pre-reacted TiC diluent addition.

system used in this work [23]. A systematic shift in the thermal profiles to longer times, an increase in time between thermal spikes for the two cells and lower adiabatic temperatures with dilution are all indicative of the slower reaction propagation caused by dilution.

Retardation of reaction propagation kinetics with increasing dilution to 30% is also indicated in a plot of SHS velocity versus dilution level (Fig. 6). The velocity for undiluted mixtures was noted to be more than double that of 30% dilution, decreasing from about 10 to 4 mm s^{-1} for these levels. No reaction at 50% dilution was also predicted by the algorithm. This was because the low adiabatic reaction temperature for 50% dilution addition (1800 K) is well below the ignition temperature of the Ti–C reaction (1940 K), which does not allow the reaction to be self-sustaining in nature. Experimental observations of no reaction at

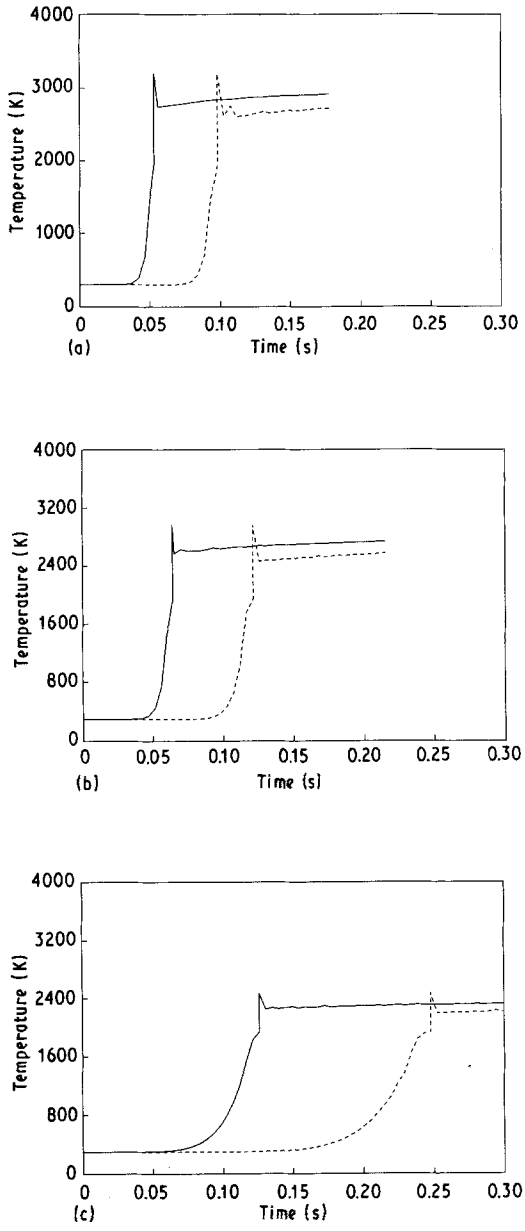

Figure 5 Illustration of reduction in propagation velocity with dilution through temperature–time profile predictions from two fixed cell locations (Nos E15 and E25, 0.5 mm apart) at (a) 0, (b) 10 and (c) 30% diluent levels: (——) E15, (– – –) E25.

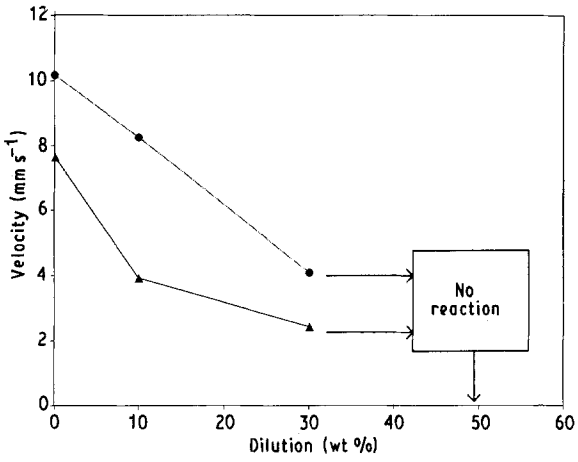

Figure 6 (●) Predicted and (▲) experimental measurements of dilution effects on reaction propagation kinetics, showing a decrease in velocity with increasing dilution to 30%, and absence of reaction at 50% dilution.

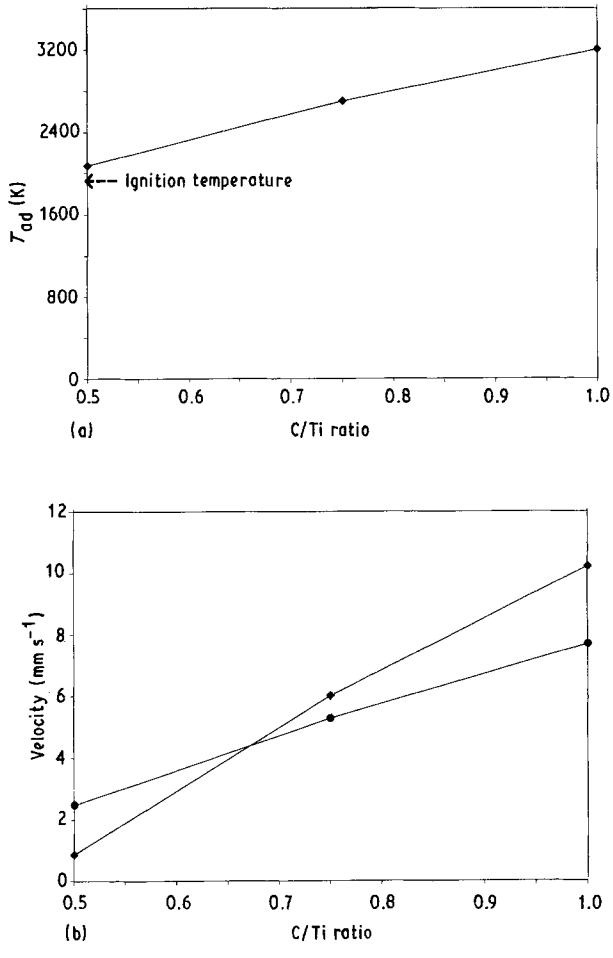

Figure 7 Influence of initial powder stoichiometric ratio on (a) predicted adiabatic temperature and (b) (◆) predicted versus (●) measured SHS reaction velocity for 1:1 to 1:0.5 Ti:C ratios.

this dilution level, and measured reaction velocities of 8 to 2 mm s^{-1} for 0–30% dilution, in fact indicate excellent qualitative and quantitative agreement with trends predicted by the model (Fig. 6). This trend is also in good agreement with observations made by Kottke *et al.* [12] and other Russian literature, as illustrated in the review paper by Munir and Tamburini [1].

The initial stoichiometric ratio of Ti:C is predicted to have an effect on adiabatic temperature and reaction velocities, as observed for dilution (Fig. 7). The decrease in these variables was due to a lowering of the heat of reaction caused by smaller amounts of reacting powders and the presence of unreacted powder diluents within the final product phase. The maximum adiabatic reaction temperature predicted was 3200 K for a 1:1 Ti:C ratio, which fell to a little above 2000 K for a reactant ratio of 1:0.5. Corresponding velocity values were noted to continuously decrease from 10 to about 1 mm s^{-1} for stoichiometric versus off-stoichiometric conditions. The simulation of reaction velocity again showed good agreement with experimental measurements of this parameter made in this work, though the predicted trend of velocity decrease with off-stoichiometry conditions was sharper than that observed experimentally.

3.2. Preheat temperature effects on SHS

Preheat was modelled to accelerate the SHS reaction propagation kinetics through the temperature range from ambient to 1000 °C. This acceleration in reaction propagation with initial compact temperature is best illustrated in a plot of SHS velocity versus preheat temperature, as shown in Fig. 8. The figure illustrates that the velocity increases from 10 mm s^{-1} at room temperature to 25 mm s^{-1} at 1000 °C. The simulation shows excellent agreement with experimental measurements of increasing velocity from 8 to about 20 mm s^{-1} up to 850 °C, though a sharp decrease in velocity to 15 mm s^{-1} measured at 950 and 1000 °C shows a poor match with the predicted trends (Fig. 8).

The increase in SHS reaction velocity with preheating to 200 °C was modelled to be caused by a combined effect of increased adiabatic temperature (3200–3290 K) and increased initial cell temperature due to preheating (Fig. 9). Beyond 200 °C the adiabatic reaction temperature was predicted to be constant at 3290 K, which is the melting point of TiC, and only an increase in the melt fraction from 0 to 60% was modelled to occur with further preheating to 1000 °C. The increase in velocity measured from 200 to 850 °C thus appears to be only due to an increase in the initial cell temperature, though the melt may also provide a contribution to the change in the reaction kinetics.

The decrease in experimentally measured velocity above 850 °C is possibly due to a change in powder characteristics at 950 and 1000 °C. For example, Ti undergoes a phase transformation from α-h c p to β-b c c phase at 893 °C [27] which can alter the thermal and chemical properties of the initial reactant powder, which may influence the process. Although the model considers the phase transformation in the computation of adiabatic reaction temperatures, the thermal conductivity properties of the α and β phases were not available, and may lead to the differences predicted at high preheat temperatures. Further, the excessive product melting (up to 60%) at high initial compact temperatures can contribute to the heat transfer process and yield additional differences between model and experiment.

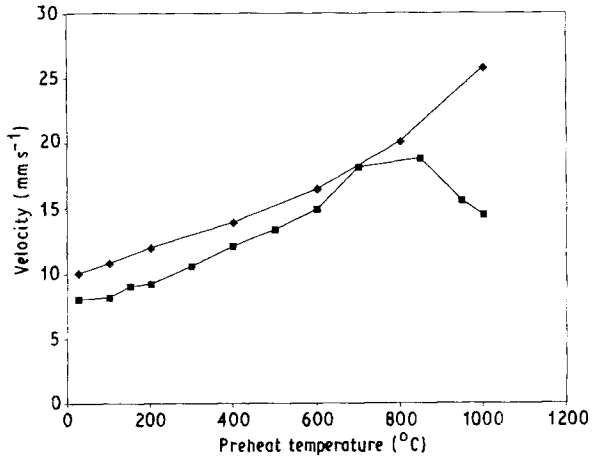

Figure 8 Preheat effects on acceleration in (◆) predicted and (■) measured SHS reaction propagation velocity.

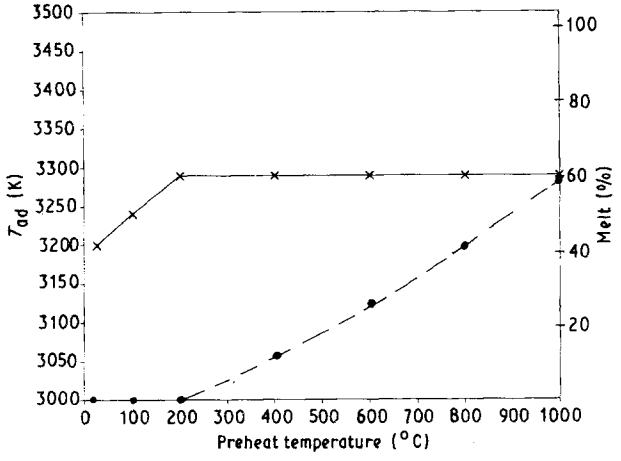

Figure 9 Influence of preheat on predicted values of (×) adiabatic reaction temperature and (●) product TiC melt fraction for preheat temperatures from room temperature to a maximum of 1000 °C.

3.3. Particle size and packing density effects on SHS

Modelling of particle size effects on SHS reaction velocity was carried out by assuming the mesh size to be that of the powder dimension. Predicted results indicated a continuous decrease in reaction velocity with increasing particle size (Fig. 10). Since the size was only simulated to affect the heat transfer rate, the effect could be understood from the effect of this parameter on the reaction propagation process. For example, if one considers larger cell dimensions, the ignition of a cell by heat transfer from its previous cell at the adiabatic temperature depends on the time for that cell to heat up from room temperature to the ignition temperature by conduction Instead, smaller mesh dimensions split up the distance for heat transfer, and accelerate the propagation process by continuous rapid ignition of the smaller cells to the adiabatic temperature. It should, however, be noted that as the particle size increases, reaction and diffusion kinetics also start playing an important role in the process, and can produce a larger influence on velocities

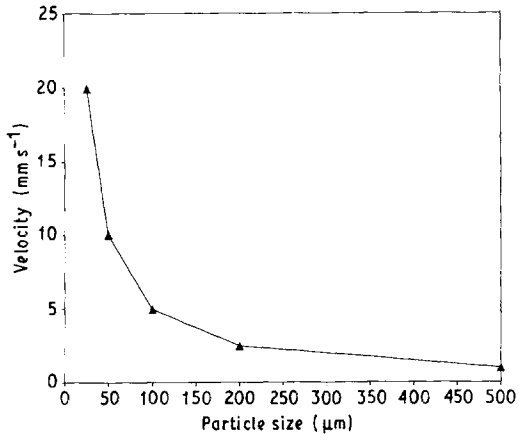

Figure 10 Model predictions of particle size effects on SHS reaction velocity, indicating a continuous decrease in velocity with increasing size.

than those modelled in this work. Despite this limitation, trends predicted by the model show reasonable agreement with those indicated in the review paper by Munir and Tamburini [1].

An increase in the packing density from 45 to 85% was empirically evaluated to produce a mass density increase from about 1700 to 3200 $kg\,m^{-3}$, a parallel thermal conductivity increase from 0.17 to 1.8 $W\,m^{-1}\,K^{-1}$ and perpendicular thermal conductivity from 0.25 to 4.4 $W\,m^{-1}\,K^{-1}$, though the thermal conductivity effect was found to dominate over that of the mass density. Also, since a 40×1 modified two-dimensional mesh system was used, only parallel thermal conductivity increases influenced the heat flow process. The predicted velocity was found to increase with increasing packing density, since at lower density (and conductivity), the thermal energy is confined close to the ignition element, resulting in slow ignition and reaction velocities. As the packing density, conductivity and heat transfer rate increased, the velocity increased from about 3 $mm\,s^{-1}$ at 45% density to about 12 $mm\,s^{-1}$ at 85% density, thus producing a fourfold increase in velocity over the range of packing densities simulated (Fig. 11a). The predicted velocity of 10 $mm\,s^{-1}$ at about 55% packing density was slightly higher than that of 8 $mm\,s^{-1}$ measured experimentally, thus indicating good agreement between model and experiment at this density level. Since, in practice, it is difficult to achieve the entire range of packing density, model performance for other packing density values was evaluated by comparing with a similar simulation developed by Kottke and co-workers [20, 21]. Both models showed similar trends and agreement in predicted velocity as a function of packing density, though the values in this work were lower than those of Kottke and co-workers, especially at higher packing levels (Fig. 11b).

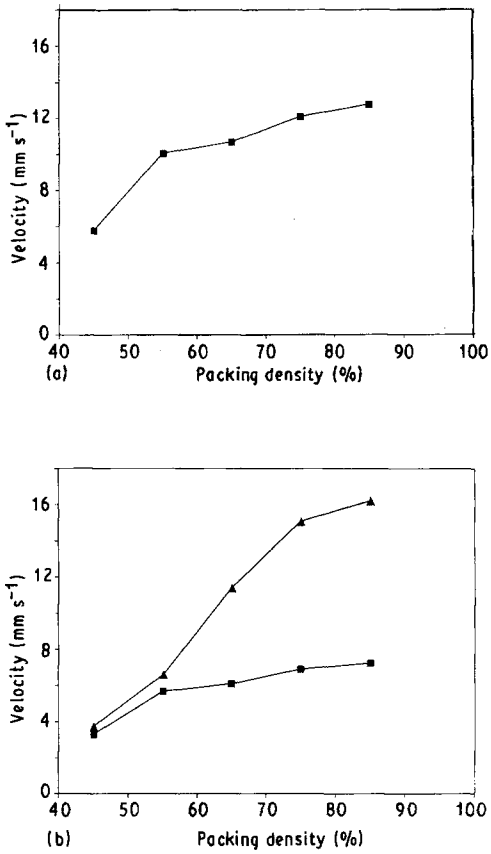

Figure 11 Illustration of increase in predicted SHS velocity over the range of green compact packing densities from 45 to 85%, as modelled (a) in this research and (b) in the work of Kottke and co-workers [20, 21]. It should be noted that the plot of (a) was modelled assuming a powder particle size of 50 μm to match other simulations developed in this work, while the size used to predict plots in (b) was 85 μm to compare with a similar size used by Kottke and co-workers.

4. Summary and conclusions

A dynamic, finite-difference model developed to evaluate titanium carbide (TiC) ceramic processing by self-propagation high-temperature synthesis (SHS) has revealed the following:

1. Material and process parameters have a significant influence on SHS reaction propagation kinetics.
2. Addition of inert pre-reacted TiC diluents to the initial Ti–C reactant mixture and the use of off-stoichiometric Ti:C ratios tend to decrease the SHS reaction velocities.
3. Increasing compact preheat temperatures, lowering powder particle sizes and raising compact packing densities cause a significant increase in SHS reaction propagation kinetics.
4. The effects of these initial material and process conditions are due to their influence on adiabatic reaction temperatures and heat transfer patterns produced during the process.
5. Model results are in agreement with results obtained from suitably designed experimental studies on dilution, stoichiometry and preheat temperature effects on SHS velocity, and other literature data on packing-density and particle-size effects on this parameter.

Acknowledgements

The authors would like to thank Dr A. Niiler, Ballistics Research Laboratory, for valuable discussions. Funding for this research was obtained from the DARPA Balanced Technology Initiative and Ballistics Research Laboratory, Maryland by the Center for Explosives Technology Research, New Mexico Tech through a subcontract with the University of California at San Diego. The work was also funded in part by the Research Council at New Mexico Tech and DOD Grant DN-009, Defense Logistics Agency, Directorate for Stockpile Management administered by the University of Texas at El Paso Institute for Manufacturing and Materials Management.

References

1. Z. A. MUNIR and U. A. TAMBURINI, *Mater. Sci. Rep.* **3** (1989) 278.
2. H. C. YI and J. J. MOORE, *J. Mater. Sci.* **25** (1990) 1159.
3. J. D. WALTON Jr and N. E. POULOS, *J. Amer. Ceram. Soc.* **42** (1959) 40.
4. B. H. RABIN, G. E. KORTH and R. L. WILLIAMSON, *ibid.* **73** (1990) 2156.

5. Y. MIYAMOTO and M. KOIZUMI, "Combustion and Plasma Synthesis of High Temperature Materials", presented at the International Symposium on Combustion and Plasma Synthesis of High Temperature Materials, American Ceramic Society, San Francisco, October 1988, edited by Z. A. Munir and J. B. Holt (VCH Publishers, NY, 1990) pp. 163–169.
6. A. NIILER, L. J. KECSKES, T. KOTTKE, P. H. NETHERWOOD Jr and R. F. BENCK, "Explosive Consolidation of Combustion Synthesized Ceramics", Technical Report BRL-TR-2951 (Ballistic Research Laboratory, Aberdeen Proving Ground, Maryland, 1988).
7. J. B. HOLT, *Mater. Bull.* **12(7)** (1987) 60.
8. Y. MIYAMATO, *Ceram. Bull.* **69** (1990) 686.
9. K. A. PHILPOT, Z. A. MUNIR and J. B. HOLT, *J. Mater. Sci.* **22** (1987) 159.
10. J. TRAMBUKIS and Z. A. MUNIR, *J. Amer. Ceram. Soc.* **73** (1990) 1240.
11. A. D. BRATCHIKOV, A. G. MERZHANOV, V. I. ITIN, V. M. KHACHIN, E. F. DUDAREV, V. E. GYUNTER, V. M. MASLOV and D. B. CHERNOV, *Sov. Powder Metall. Met. Ceram.* **19** (1980) 5.
12. T. KOTTKE, L. J. KECSKES and A. NIILER, "Control of TiB_2 SHS Reactions by Inert Dilutions and Mechanical Constraint", Memorandum Report BRL-MR-3793 (Ballistic Research Laboratory, Aberdeen Proving Ground, Maryland, 1989).
13. J. B. HOLT and Z. A. MUNIR, *J. Mater. Sci.* **21** (1986) 251.
14. J. B. HOLT, D. D. KINGMAN and G. M. BIANCHINI, *Mater. Sci. Engng* **71** (1985) 321.
15. M. E. MULLINS and E. RILEY, *J. Mater. Res.* **4** (1989) 408.
16. A. P. HARDT and R. W. HOLSINGER, *Combust. & Flame* **21** (1973) 91.
17. A. H. ADVANI, R. HEAPS and N. N. THADHANI, Unpublished work, Center for Explosives Technology Research, New Mexico Tech. (1990).
18. A. G. MERZHANOV and A. E. AVERSON, *Combust. & Flame* **16** (1971) 89.
19. A. P. HARDT and P. V. PHUNG, *ibid.* **21** (1983) 77.
20. T. KOTTKE, L. J. KECSKES and A. NIILER, "Combustion and Plasma Synthesis of High Temperature Materials", presented at the International Symposium on Combustion Synthesis of High Temperature Materials, San Francisco, October 1988, edited by Z. A. Munir and J. B. Holt (VCH Publishers, NY, 1990) pp. 238–245.
21. T. KOTTKE and A. NIILER, "Thermal Conductivity Effects on SHS Reactions", Technical Report BRL-TR-2889 (Ballistic Research Laboratory, Aberdeen Proving Ground, Maryland, 1988).
22. R. BEHRENS and G. P. HANSEN, in Proceedings of DARPA/Army SHS Symposium on Materials Processing by Self-Propagating High Temperature Synthesis, Daytona Beach, Florida, October 1985, edited by K. A. Gabriel, S. G. Wax and J. W. McCauley, MTL Publication no. SP87-3 (Materials Technology Laboratory, Watertown, MS) pp. 43–62.
23. A. H. ADVANI, N. N. THADHANI, H. A. GREBE, R. HEAPS and C. COFFIN, *Scripta Metall.* **25** (1991) 1447–1452.
24. E. A. BRANDES (ed.) "Smithells Metals Reference Book", 6th Edn (Butterworths, London, 1983) pp. 8-1–8-43.
25. Y. S. TOULOUKIAN (ed.), "Thermophysical Properties of High Temperature Solid Materials" (Macmillan, New York, 1967) pp. 182–185.
26. F. P. INCROPERA and D. P. DEWITT, "Fundamentals of Heat Transfer" (Wiley, New York, 1981) pp. 763–769.
27. M. W. CHASE Jr, C. A. DAVIES, J. R. DOWNEY Jr, D. J. FRURIP, A. A. McDONALD and A. N. SYVERUD (eds), "JANAF Thermochemical Tables", 3rd Edn, Parts I and II (American Chemical Society and the American Institute of Physics for National Bureau of Standards, Michigan, 1985) pp. 535, 640–642 and 1818–1823.

Received 27 February
and accepted 1 July 1991